Article

Patterns

Complex Network Representation of the Structure-Mechanical Property Relationships in Elastomers with Heterogeneous Connectivity

Graphical Abstract

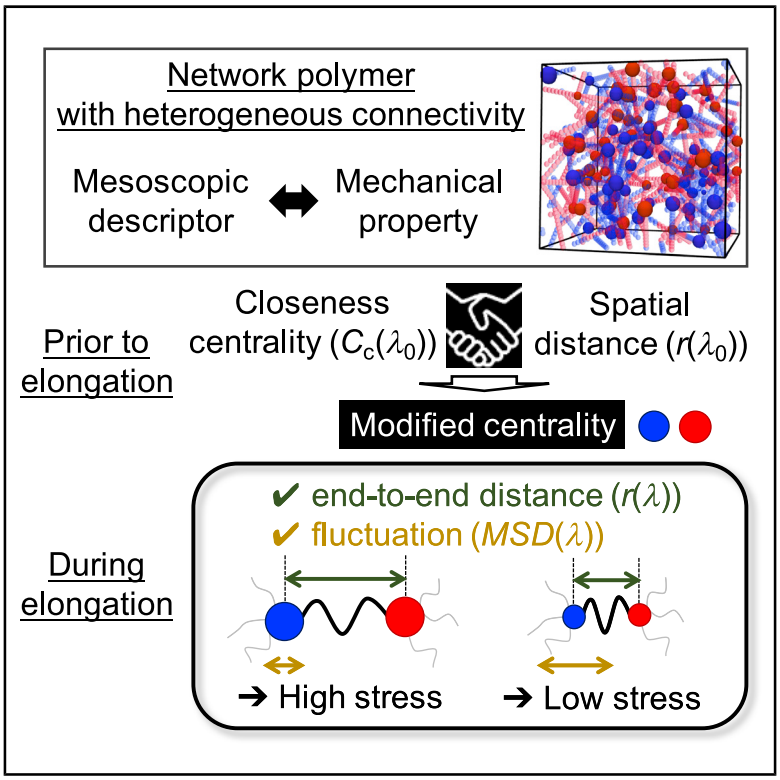

Highlights

- Developed network indicator with both connectivity and spatial distance between nodes
- Network indicator used as a mesoscopic descriptor of network polymers or elastomers
- Mesoscopic descriptors universally represented certain parameters related to stress
- Incorporating spatial distance into closeness centrality is useful for other materials

Authors

Yoshifumi Amamoto, Ken Kojio, Atsushi Takahara, Yuichi Masubuchi, Takaaki Ohnishi

Correspondence

y-amamoto@ms.ifoc.kyushu-u.ac.jp (Y.A.),
ohnishi.takaaki@i.u-tokyo.ac.jp (T.O.)

In Brief

Network polymers comprise materials encountered in our daily life, such as foam rubbers, adhesions, and rubber tires. The mechanical properties of network polymers or elastomers depend on the network structure; however, the heterogeneity of the connectivity is difficult to evaluate quantitatively. A mesoscopic descriptor of network polymers was developed to describe the structure-mechanical property relationships based on closeness centrality, a complex network indicator. The mesoscopic descriptor with both topological and spatial information universally represented parameters that determine the mechanical properties.

Amamoto et al., 2020, Patterns *1*, 100135
November 13, 2020 © 2020 The Author(s).
https://doi.org/10.1016/j.patter.2020.100135

CellPress

Patterns

CellPress
OPEN ACCESS

Article

Complex Network Representation of the Structure-Mechanical Property Relationships in Elastomers with Heterogeneous Connectivity

Yoshifumi Amamoto,[1,2,3,4,*] Ken Kojio,[3] Atsushi Takahara,[3] Yuichi Masubuchi,[2] and Takaaki Ohnishi[1,*]
[1]Graduate School of Information Science and Technology, The University of Tokyo, 7-3-1 Hongo, Bunkyo-ku, Tokyo 113-8656, Japan
[2]Department of Materials Physics, Nagoya University, Furo-cho, Chikusa-ku, Nagoya 464-8603, Japan
[3]Institute for Materials Chemistry and Engineering, Kyushu University, 744 Motooka, Nishi-ku, Fukuoka 819-0395, Japan
[4]Lead Contact
*Correspondence: y-amamoto@ms.ifoc.kyushu-u.ac.jp (Y.A.), ohnishi.takaaki@i.u-tokyo.ac.jp (T.O.)
https://doi.org/10.1016/j.patter.2020.100135

THE BIGGER PICTURE Complex network science has contributed to extracting essential parameters from network structure and has been applied in social, geographical, computer, and biological sciences. On the other hand, in materials science, some materials possess a network structure that determines their properties. Because both connectivity and spatial distance are significant factors in materials, utilizing a combined descriptor to explain their properties could be important. In this study, we demonstrate that the descriptor with both connectivity and spatial distance prior to elongations universally represented some parameters related to mechanical properties during elongation, which enabled us to interpret the role of each node. Recently, there have been significant attempts to develop new materials by methods in data science such as materials informatics. Thus, our approaches could contribute in the future to the development of materials with network structures in an interpretable manner.

Proof-of-Concept: Data science output has been formulated, implemented, and tested for one domain/problem

SUMMARY

The complicated structure-property relationships of materials have recently been described using a methodology of data science that is recognized as the fourth paradigm in materials science. In network polymers or elastomers, the manner of connection of the polymer chains among the crosslinking points has a significant effect on the material properties. In this study, we quantitatively evaluate the structural heterogeneity of elastomers at the mesoscopic scale based on complex network, one of the methods used in data science, to describe the elastic properties. It was determined that a unified parameter with topological and spatial information universally describes some parameters related to the stresses. This approach enables us to uncover the role of individual crosslinking points for the stresses, even in complicated structures. Based on the data science, we anticipate that the structure-property relationships of heterogeneous materials can be interpretatively represented using this type of "white box" approach.

INTRODUCTION

The material properties rely not only on the chemical structure or composition of compounds but also on the mesoscopic structure determined in the processes. The mesoscopic structure of materials, which often indicates complicated geometries, such as in-phase separation, polycrystalline structure, and dispersion state of particles, governs their properties. Because of the complicated structure, it is difficult to describe the material properties directly because the data of mesoscale structures in materials are sometimes spatial and multi-dimensional in nature. Therefore, essential parameters of the mesoscopic structure to explain the properties of the materials have been obtained using several methods, such as fractal dimension, persistent homology, and polyhedral combinatorics.[1,2] Recently, there have been some attempts to extract structural descriptors on a

This is an open access article under the CC BY-NC-ND license (http://creativecommons.org/licenses/by-nc-nd/4.0/).

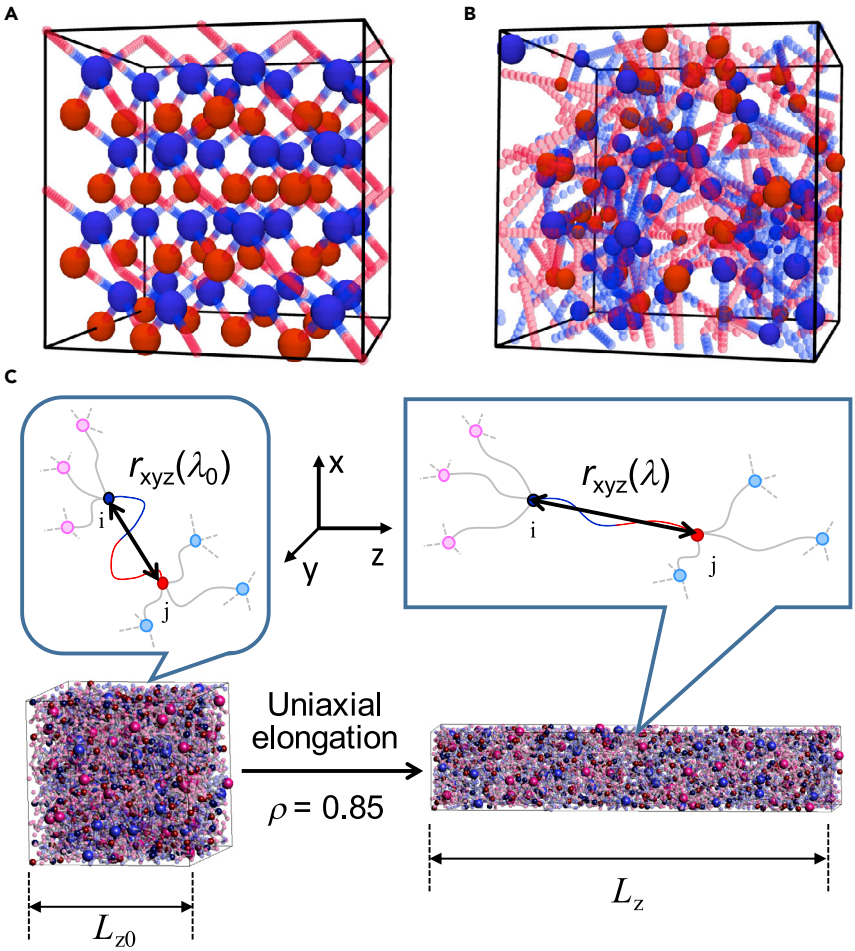

Figure 1. Heterogeneous Structure of Elastomer Based on Network Centrality and End-To-End Distance under Uniaxial Elongation

(A and B) Complex network representations of (A) homogeneous and (B) heterogeneous elastomers. The size of the nodes represents the value of closeness centrality treated with min-max normalization.

(C) In this study, the end-to-end distance $r_{xyz}(\lambda)$ is defined as the time-average of the Euclidean distance between two pairs of crosslinking points connected by one chain in an elongated state.

mesoscopic scale based on data science, which enables the handling of more complex structures.[3] For example, convolutional neural networks recognize some important shapes from images with structural information, while the regression of a property generally indicates a non-linear relationship.[4,5] Furthermore, some algorithms in data science are expected to extract essential parameters that supply a simple relationship between the structural descriptors and the properties. Thus, based on data science, the establishment of a method that obtains descriptors on a mesoscopic scale is highly desirable for describing structure-property relationships.

An elastomer is typically a material with a complicated mesoscopic structure because of its crosslinked structure, considering that the polymer chains are heterogeneously connected among the crosslinking points, thereby possibly affecting its mechanical properties.[6–10] Elastomers are crosslinked polymers in rubber states where the polymer chains are connected by crosslinked points to form a network structure. Moreover, elastomers are applied to rubbers, tires, foam rubbers, adhesives, and extracellular matrices, among others. In the rubber states of elastomers, although the positions of the polymer chains change like liquid, the materials indicate elasticity rather than flowability, owing to its network structure. Many physical models that indicate the structure-property relationships of elastomers or gels have been successfully constructed, mainly based on neo-Hookean solids[11–18] in consideration of connectivity, entanglement, and dangling chain.[19–27] These methods generally focus on relatively small regions around the neighboring crosslinking structure. In contrast, complex networks, one of the tools of data science,[28–31] have recently been utilized to extract the descriptors of materials with a network structure.[32,33] Thus, it was expected that complex network science could extract the descriptors of elastomers on a larger scale[34] and could describe their properties simply, thereby enabling the discussion of hierarchical and heterogeneous structures.

In this study, we extract the mesoscopic descriptors of elastomers comprised of monodisperse polymer chains and heterogeneous connectivity to explain their mechanical properties based on a complex network. A unified descriptor reflecting both the topological and spatial information of the elastomers for each crosslinking point was developed based on the closeness centrality, which can be applied to represent the heterogeneity of materials on the mesoscopic scale (Figures 1A and 1B). Hence, we discuss the effect of the descriptor on the end-to-end distance, the fluctuations of the crosslinked points under elongation, and shear modulus (Figure 1C).

RESULTS AND DISCUSSION

Preparation and Structure of the Elastomers

To construct elastomers with several connectivities, we compared homogeneous and heterogeneous network structures through coarse-grained molecular dynamics simulations using Kremer-Grest bead-spring models because it is difficult to check experimentally.[35,36] Diamond-like as well as synthetically and randomly crosslinked elastomers were designed in the simulations to represent homogeneous and heterogeneous networks, respectively (Figure S1). Networks crosslinked by two kinds of polymers with four branching polymer chains as A4+B4 types were examined (Figure 2A). In all cases, the particle number between the crosslinking points was fixed at $N_{xlp\text{-}xlp}$ = 22, unless otherwise mentioned, because the short chains resulted in relatively small entanglements and elongation rate

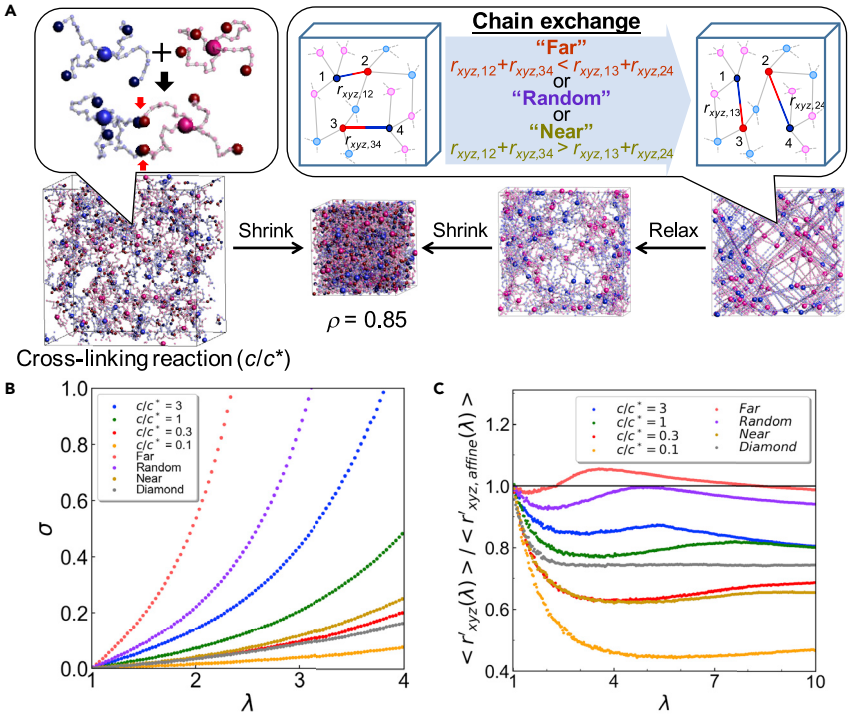

Figure 2. Preparation and Uniaxial Elongation of Synthetically and Randomly Crosslinked Elastomers

(A) Preparation of elastomers by chain-end crosslinking of star prepolymers at several concentrations (left: c/c^* = 3, 1, 0.3, and 0.1) and by chain exchanges between crosslinking points with/without distance conditions (right: far, random, and near).

(B) Stress-strain curves of elastomers under uniaxial elongation.

(C) Relationship between $<r'_{xyz}(\lambda)>/<r'_{xyz,affine}(\lambda)>$ and λ of elastomers, in which $r'_{xyz,affine}(\lambda)$ is estimated by $r'_x(\lambda_0)^*\lambda^{0.5} + r'_y(\lambda_0)^*\lambda^{0.5} + r'_z(\lambda_0)^*\lambda$. The black line corresponds to affine deformations. Blue, green, red, and orange circles represent the synthetically crosslinked polymers prepared at c/c^* = 3, 1, 0.3, and 0.1, respectively. Pink, purple, yellow ochre, and gray circles represent the far, random, and near conditions and the diamond-like network, respectively.

effects on the stress-strain curves.[37] The diamond-like elastomer was constructed as a homogeneous network without entanglement for comparison with other heterogeneous networks. The crosslinking points in the diamond-like elastomers were located at the position of carbon in the diamond lattice, and the polymer chains were connected through bonds similar to carbon-carbon bonds (Figure S1A).

A synthetically crosslinked elastomer was produced via crosslinking reactions at the chain ends of two types of complementarily reactive 4-arm star precursor polymers with 11 beads for each arm because it was easy to unify the number of beads between crosslinking points, as compared with chain-growth polymerizations. In this case, one type of star polymer must connect to the other types (Figure 2A).[38–40] To examine the effect of connectivity, we investigated crosslinking reactions at several concentrations, and made the resulting cells smaller, up to ρ = 0.85 in size, to be able to conduct uniaxial elongations at the same densities.[12] With an increase in the crosslinking concentration (c/c^*, where c refers to the crosslinking concentration and c^* pertains to the overlap concentration), the crosslinking reaction rates accelerated because of the collision probability (Figure S2A). The conversions exceeded 95% (Figure S2B), thereby indicating that these polymers possessed almost the same crosslinking density after shrinkage. Furthermore, the star polymers were connected to form a single network in $c/c^* \geq 0.1$ (Figure S2A). It is important to note that the number of defects in a network, such as self-looping or dangling chains, were significantly fewer in number due to the use of complementary reactive polymers and high conversions.

The process might be more inclined toward synthetically prepared elastomers in terms of their connectivity in a complex network because crosslinking reactions or the formation of links occur only within a limited space due to the length of the arms. Thus, we fabricated a randomly crosslinked network through artificial means to determine the generality of the results. The randomly crosslinked elastomers exhibited two types of crosslinking points at random positions in a simulation box, and the polymer chains between them with branching number f = 4 were connected (Figure S1C). The polymer chains in the random network were exchanged with or without distance conditions, including far, random, and near conditions (Figure 2A). Because chains with shrunken and extended bonds were formed, the networks were quite tight. Therefore, the polymer chains were relaxed without interchain interactions. Thereafter, the simulation boxes decreased in size through interchain interactions, and uniaxial elongations were carried out through interactions wherein a reconnection was not applied. Thus, the crosslinking density and amount of branching were almost the same for all the elastomers.

To confirm the effect of the preparation methods, we evaluated the network structure through simple visualization and radial distribution functions (RDFs) under an isotropic expansion of the compressed cells. In the graphic illustration, the network prepared under c/c^* = 1 seems to be relatively homogeneous, which was likewise confirmed through a broad plateau region in the RDF (Figures S3A and S3B). In the case of c/c^* = 3, globally connected polymer chains with some condensed regions were observed, whereas the polymers prepared with c/c^* = 0.1 led to the formation of notable condensed parts and empty spaces (Figure S3A). In the RDFs, characteristic peaks were observed in small and medium regions for c/c^* = 3 and 0.1, respectively, thereby supporting the formation of some clusters (Figure S3B). Furthermore, the number of loop chains or polymer chains with common crosslinking points increased with a decrease in the reaction concentration (Figure S3C). Considering these results, at low concentrations the crosslinking reactions in local regions should result in the formation of large clusters with numerous loops connected by bridge chains. In contrast, at high concentrations the polymer chains can reach distant regions, thereby

forming globally connected chains with fewer loops and more knots. Under overlapping concentrations, star polymers can be connected in a relatively homogeneous manner because a polymer chain can make suitable contact with the surrounding polymers. For randomly crosslinked elastomers, the near conditions showed a peak in the RDF, indicating the formation of clusters, such as the low concentration in synthetically crosslinked elastomers (Figure S3D). These results indicate that the connectivity of the elastomers clearly depends on the reaction concentration and the exchange condition.

Uniaxial Elongation of Elastomers

The effects of the network structure on the mechanical properties were analyzed, based on the uniaxial elongation of the crosslinked polymers as compared with the elastic model. There have been many models used to describe the entropy elasticity of elastomers or gels based on a neo-Hookean solid. An affine network model is the most basic elastic model of elastomers or gels, whereby an affine deformation of polymer chains including crosslinking points is assumed. The stress is described by two parameters, number of polymer chains per unit volume (ν) and elongation ratio (λ), as indicated by

$$\sigma = \nu k_B T \left(\lambda^2 - \lambda^{-1}\right).$$

Therefore, the stress increased with an increase in the number of crosslinked polymer chains in this model. If the deformation of the polymer chains deviates from the affine deformation, the stress decreases because the decrease in entropy due to elongation is less. In the phantom network model, the fluctuation of the crosslinking points is considered, while the affine deformation of crosslinking points itself is not assumed (see Equation 5 in Supplemental Information). The stress increases with increasing number of polymer chains connected to crosslinking points (f) because the fluctuation of crosslinking points was suppressed. In this study, $f = 4$, so the stress of the affine network model is twice as large as that of the phantom network model. It should be noted that these models do not consider the connectivity of polymer chains. In our research, ν and f were almost identical in all elastomers, which enabled us to discuss the effect of connectivity. Therefore, the end-to-end distance between crosslinking points connected by a polymer chain $r_{xyz}(\lambda)$ and mean square displacement of cross-linking points ($MSD_{xyz}(\lambda)$) for all directions in each λ under elongations are evaluated as parameters that determine the level of stress.

In the case of synthetically crosslinked elastomers, the stresses under uniaxial elongation clearly depended on the crosslinking concentrations, and polymers prepared at high concentrations afforded high moduli (Figure 2B). In a Mooney-Rivlin plot, where the black line indicates a phantom network model, high-modulus polymers achieved extended chain effects at low elongation ratios (Figure S4A). Interestingly, crosslinking reactions at the overlap concentration ($c/c^* = 1$) produced polymers with almost the same stress as those in the phantom network model, i.e., up to $\lambda \approx 2.5$ (Figure S4A), as previously observed in a real gel, thereby suggesting that our simulation model could represent a real system.[38] In the case of $c/c^* = 0.1$, a broad plateau region was confirmed. This phenomenon is known as superelasticity.[41] However, the modulus of the elastomer prepared for $c/c^* = 3$ was twice that of a phantom network model and was close to that of an affine network model. When elongation was conducted without an interchain interaction or Lennard-Jones potential, the difference in the stress was not pronounced, thereby indicating that an entanglement or knot did not appear essential in the stress-strain curves (Figure S4A). When the polymer chains were longer, such as when $N_{xlp\text{-}xlp} = 62$, other effects, such as an entanglement, appeared in the Mooney-Rivlin plot in $\lambda^{-1} > 0.5$, and the only effect of connectivity cannot be discussed (Figure S4B). This study dealt with crosslinked polymers in the rubber state for which the entropic elasticity was confirmed by the temperature dependence of the shear modulus (Figure S4C). Almost no hysteresis was observed at the low elongation rates at which we carried out the elongation (Figure S5). Therefore, the difference in the stresses of the rubber elasticity could be derived from the network structure. The stress-strain curves of randomly crosslinked elastomers showed a dependence on the exchange conditions (Figure 2B). The near condition was the one closest to that of the reactively prepared elastomers among the randomly crosslinked networks (Figure 2B). Specifically, far conditions enabled higher stresses with a deviation from the plateau in the early stages due to an extended chain effect, whereas near conditions lowered stresses while maintaining a wide plateau (Figures 2B and S4D).

The differences in stress-strain curves could be derived from the deviation from the assumptions in the neo-Hookean solid, such as affine deformation.[42] Therefore, the ratio of the end-to-end distance at each elongation step ($r'_{xyz}(\lambda)$) to the theoretical end-to-end distance calculated from the initial end-to-end distance ($r'_{xyz,affine}(\lambda)$) was plotted against the elongation ratio (λ), whereby the horizontal line at 1 corresponds to the theoretical affine deformation (Figure 2C). In synthetically crosslinked elastomers, with a decrease in the crosslinking concentration, the expansion of the end-to-end distance deviated from the affine deformation. With regard to randomly crosslinked polymers, the plots obtained under random and far exchange conditions nearly coincided with the theoretical line (Figure 2C). However, the end-to-end distance was below the theoretical line under near conditions (Figure 2C), thereby indicating the delayed expansion of the chains. The stresses decreased when the deviation from the affine deformations increased. Interestingly, after elongation to a certain extent, plateau regions appeared in all elastomers. These results are consistent with those of a previous report stating that a heterogeneous network does not always satisfy affine deformation, which depends on how the polymer chains are connected.[42]

Quantification of the Heterogeneous Network Structure for the Mechanical Properties

Our goal is to predict the mechanical properties during elongation using mesoscopic structural descriptors prior to elongations (λ_0). This enables us to predict the stress merely by the initial mesoscale structure descriptors without elongation. Therefore, the selection of mesoscopic descriptors is key to describing the mechanical properties. Thus, we estimated the time-average initial end-to-end distance ($r_{xyz}(\lambda_0)$) and closeness centrality ($C_c(\lambda_0)$) as mesoscopic descriptors with spatial or topological information prior to elongation. The initial end-to-end distance and

closeness centrality are estimated as the average for a pair of nodes or two crosslinking points connected by a single chain. The closeness centrality is one of the indicators of a complex network and is the reciprocal of the sum of the links of the shortest paths between any node and all other nodes, in which nodes and links are composed of the crosslinking points and connecting chains, respectively.[28,29] It represents the effectiveness of a crosslinking point in terms of its connectivity to other crosslinking points (Figure S6A). Considering that the value of the closeness centrality depends on the system size or number of crosslinking points, we can compare the values as long as the system sizes are the same. Therefore, in this study, the numbers of crosslinking points (N_{xlp}) were unified as $N_{xlp} = 100$, except for that in the diamond-like network. Thus, the mesoscopic descriptors as explanatory variables are $r_{xyz}(\lambda_0)$, $C_c(\lambda_0)$, and modified centrality, which are determined before the elongation of the elastomers. The objective variables are $r_{xyz}(\lambda)$ and $MSD_{xyz}(\lambda)$, which are the key parameters in the determination of entropic elasticity under elongations. In some cases, the shear modulus as a global stress is directly explained by $r_{xyz}(\lambda_0)$ or $C_c(\lambda_0)$, while the role of each crosslinking point cannot be evaluated in this case.

The values of both $r_{xyz}(\lambda_0)$ and $C_c(\lambda_0)$ in the synthetically crosslinked elastomers increased with increasing reaction concentrations (Figures S6B–S6E). Naturally, $r_{xyz}(\lambda_0)$ is less at a low concentration because more shrinkage of the simulation box results in a shorter end-to-end distance of the polymer chains. Interestingly, the centrality was also altered when the crosslinking concentrations were changed, which was independent of the shrinkage steps. The polymer chains in the crosslinking points prepared at higher concentrations are connected to the entire network, which leads to high centrality (Figure S3A). However, the formation of clusters in a low crosslinking concentration decreases the centrality due to the localization of the nodes in the network. In the case of randomly crosslinked elastomers, three types of polymers with nearly the same $C_c(\lambda_0)$ and different $r_{xyz}(\lambda_0)$ were obtained (Figure S7). In addition, the values of $r_{xyz}(\lambda_0)$ for the far and random conditions were higher than those of the reactively prepared elastomers, albeit $C_c(\lambda_0)$ was almost the same (Figure S7). Thus, $r_{xyz}(\lambda_0)$ and $C_c(\lambda_0)$ are possible candidates as network descriptors to explain their mechanical properties.

In a neo-Hookean solid, the initial end-to-end distance of the partial chains as polymer chains between crosslinking points or the distance between crosslinking points is assumed to follow a Gaussian distribution. Thus, the distributions of $r_{xyz}(\lambda_0)$ were evaluated in both types of crosslinked elastomers (Figure S8). The diamond-like elastomers presented a Gaussian distribution of $r_{xyz}(\lambda_0)$ based on the Kolmogorov-Smirnov test (Figure S8G). In contrast, $r_{xyz}(\lambda_0)$ adopted a Gaussian distribution in the synthetically crosslinked elastomers only for the case where $c/c^* = 0.3$ (Figure S8C). These results indicate that a heterogeneous network does not always satisfy the assumption of a neo-Hookean solid. Therefore, Spearman's rank correlation coefficient was evaluated as a non-parametric test, whereby the Gaussian assumption was not necessary.

Given that it is difficult to directly evaluate the effect of each crosslinking point on global stress, we evaluated the effects of the crosslinking points on the end-to-end distance under elongation ($r_{xyz}(\lambda)$), which is an essential parameter used to determine entropic elasticity under elongation. On the other hand, $r_{xyz}(\lambda_0)$ is a mesoscopic descriptor prior to elongation. The correlation between $C_c(\lambda_0)$ and $r_{xyz}(\lambda)$ depended on the reaction concentration and exchange conditions, and a lower concentration and a near condition resulted in a moderate correlation (Figure 3A and Table S1). The high-centrality crosslinking points were more spread out than their low-centrality counterparts, whereas the low-centrality crosslinking points can be delayed from affine deformation. The centrality of a diamond network is a single value owing to the use of a homogeneous network. In contrast, a strong correlation between $r_{xyz}(\lambda_0)$ and $r_{xyz}(\lambda)$ was observed using almost the same coefficient for all reaction concentrations and exchange conditions (Figure 3B and Table S2). It should be noted that the homogeneous diamond-like network exhibited no correlation between $r_{xyz}(\lambda_0)$ and $r_{xyz}(\lambda)$ (Figure 3B and Table S2). These results suggest that chains connecting distant crosslinking points brought these points closer to affine deformation, resulting in a long end-to-end distance as well as high moduli, making $r_{xyz}(\lambda_0)$ more effective. In contrast, at low crosslinking concentrations and near conditions, both $r_{xyz}(\lambda_0)$ and $C_c(\lambda_0)$ are effective for $r_{xyz}(\lambda)$, and the crosslinking points were unable to follow the matrix, probably because of the low centrality, which resulted in low moduli.

In the phantom network model, it is assumed that fluctuations of the crosslinking points are suppressed by increasing the amount of branching, affording high shear moduli. Therefore, the $MSD_{xyz}(\lambda)$ was evaluated for synthetically crosslinked elastomers. With increasing crosslinking concentrations, the value in the plateau region of $MSD_{xyz}(\lambda)$ decreased, thereby indicating that the fluctuation in the crosslinking points prepared at a high concentration was further suppressed (Figure S9A, $\lambda = 2$). Furthermore, the values decreased under further elongations at $\lambda = 4$ (Figure S9B). Because these tendencies of $MSD_{xyz}(\lambda)$ correspond to the stresses, we evaluated the correlation between $MSD_{xyz}(\lambda)$ and $C_c(\lambda_0)$ or $r_{xyz}(\lambda_0)$ for all crosslinked points. The correlation coefficients of $MSD_{xyz}(\lambda)$ and $C_c(\lambda_0)$ depend on the reaction concentration, and a lower concentration indicates a moderate coefficient, particularly in highly elongated states (Figure 3C and Table S3). Interestingly, the values seem to be located on a single line, except for $c/c^* = 3$, random and far conditions, for which another effect on the network structure, such as a condensed area through an isotropic expansion, should be considered (Figures 3C and S3A). This result supports the idea that the near condition might be the most representative model for a synthetically crosslinked network. In the case of $r_{xyz}(\lambda_0)$, a weak and negative correlation was confirmed, whereas the average values of the crosslinking concentrations were not plotted on a single line (Figure 3D and Table S4). These results indicate that the crosslinking points became more localized with an increase in $r_{xyz}(\lambda_0)$ or $C_c(\lambda_0)$, and the centrality was more effective for $MSD_{xyz}(\lambda)$. The crosslinked points located at the center of the network might be equivalent to the increase in the amount of branching in the phantom network model because the fluctuation in the crosslinked points was suppressed by the strong connections to other crosslinked points.

To evaluate the efficiency of current mesoscopic descriptors in terms of global stress, we examined the relationships between the averaged $C_c(\lambda_0)$ or $r_{xyz}(\lambda_0)$ and shear modulus. With an

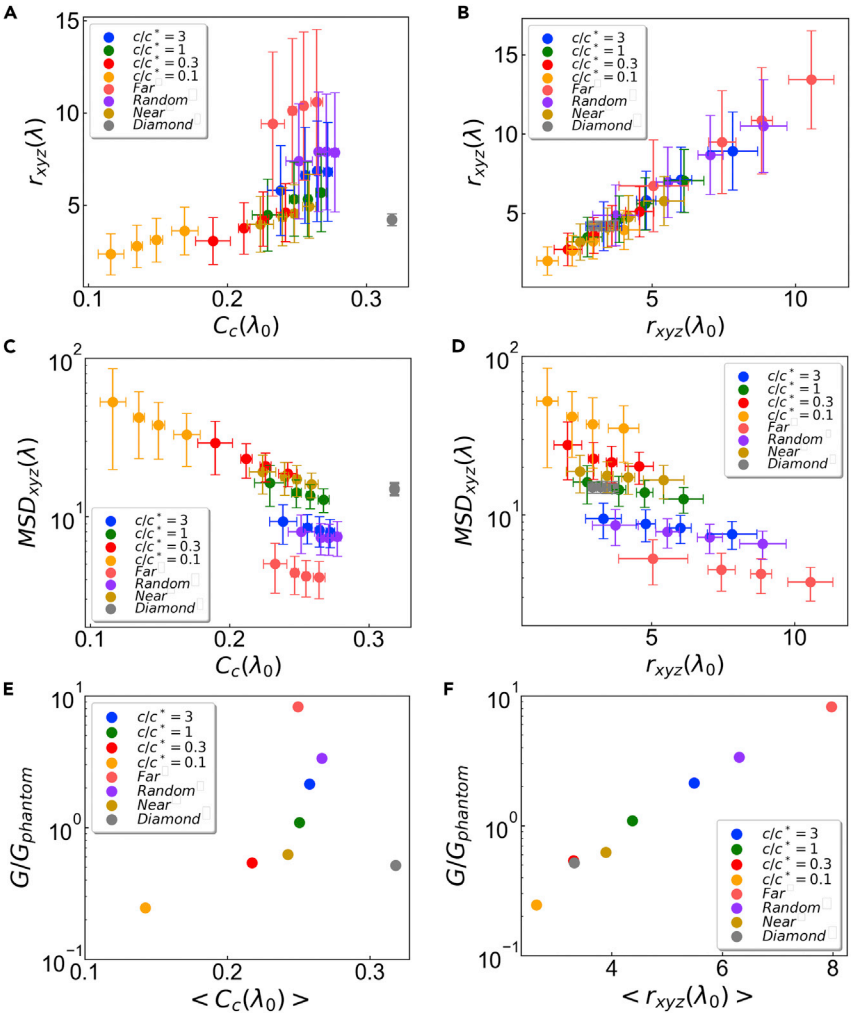

Figure 3. Effects of Initial End-To-End Distance and Closeness Centrality on End-to-End Distance under Elongation and Fluctuations of Crosslinking Points

$r_{xyz}(\lambda)$ as a function of (A) $C_c(\lambda_0)$ and (B) $r_{xyz}(\lambda_0)$, and $MSD_{xyz}(\lambda)$ as a function of (C) $C_c(\lambda_0)$ and (D) $r_{xyz}(\lambda_0)$ of the synthetically and randomly crosslinked elastomer at $\lambda = 2$. Each condition included approximately 5,000 samples ($\approx$200 polymer chains for 25 samples), which were divided into four regions based on either $r_{xyz}(\lambda_0)$ or $C_c(\lambda_0)$. Therefore, each point is an average value for approximately 1,250 samples. $G/G_{phantom}$ as a function of (E) $<C_c(\lambda_0)>$ and (F) $<r_{xyz}(\lambda_0)>$. Blue, green, red, and orange circles represent the synthetically crosslinked polymers prepared at $c/c^* = 3$, 1, 0.3, and 0.1, respectively. Pink, purple, yellow ochre, and gray circles represent the far, random, and near conditions and the diamond-like network, respectively. Error bars represent standard deviations.

increase in the average $C_c(\lambda_0)$ the shear modulus increased, except with regard to the far conditions (Figure 3E), which is consistent with the results for $r_{xyz}(\lambda)$ and $MSD_{xyz}(\lambda)$ (Figures 3A and 3C). The averaged $C_c(\lambda_0)$ does not seem to be a suitable descriptor for global stress because connectivity in the far condition was not a random network due to distance restriction in chain exchanges, which afforded low centrality. On the other hand, the averaged $r_{xyz}(\lambda_0)$ can moderately predict the shear modulus (Figure 3F). This was consistent with the result that $r_{xyz}(\lambda_0)$ in each crosslinking point could predict $r_{xyz}(\lambda)$ (Figure 3B), which determines the stress in entropic elasticity. Therefore, $r_{xyz}(\lambda_0)$ was the better descriptor for the global stress, while the improved descriptor to represent the fluctuation of crosslinking points is required.

Overall, the results obtained under synthetic and random conditions confirmed that both the initial distance between crosslinking points and closeness centrality can play key roles in determining the entropic elasticity of elastomers in heterogeneous networks. Although the initial distance seems to be more predictable than the closeness centrality for $r_{xyz}(\lambda)$, $MSD_{xyz}(\lambda)$ depends on the centrality in certain cases. When the crosslinked points obey the affine deformation, the distance under elongation mostly depends on the initial distance, regardless of the centrality. When it deviated from the affine deformation, high-centrality crosslinking points followed the movement of the entire matrix. Conversely, their low-centrality counterparts were left behind the elongations with high fluctuation, resulting in their lower contribution to the stress. Although the manner of the exchange is difficult to apply to a real elastomer, we concluded that the balance between the initial end-to-end distance and the centrality was effective, particularly for a fluctuation of the crosslinked points. In other words, both the spatial and topological information should be considered when representing the mechanical properties.

The Combined Parameters of $r_{xyz}(\lambda_0)$ and $C_c(\lambda_0)$ for a Universal Description

We attempted to establish a universal description of $r_{xyz}(\lambda)$ and $MSD_{xyz}(\lambda)$ using a descriptor that simultaneously accounts for $r_{xyz}(\lambda_0)$ and $C_c(\lambda_0)$ as spatial and topological information, respectively, because mechanical properties could be predicted without elongations. The sum of $r_{xyz}(\lambda_0)$ and $C_c(\lambda_0)$ linearly correlated with $r_{xyz}(\lambda)$, whose correlation coefficients were almost equivalent to those of $r_{xyz}(\lambda_0)$ (Figure S10A and Table S5). Although the correlation coefficients between $MSD_{xyz}(\lambda)$ and the sum of $r_{xyz}(\lambda_0)$ and $C_c(\lambda_0)$ were improved, compared with $r_{xyz}(\lambda_0)$ or $C_c(\lambda_0)$ itself it was unable to linearly describe $MSD_{xyz}(\lambda)$ (Figure S10B and Table S6).

Thereafter, we attempted to incorporate distance information into closeness centrality. In a conventional case, the weight of the link used to estimate the closeness centrality is always 1. Instead of this value, we introduced the inverse of the initial distance between the crosslinking points as a weight. Therefore, with regard to node i, the modified centrality is the reciprocal

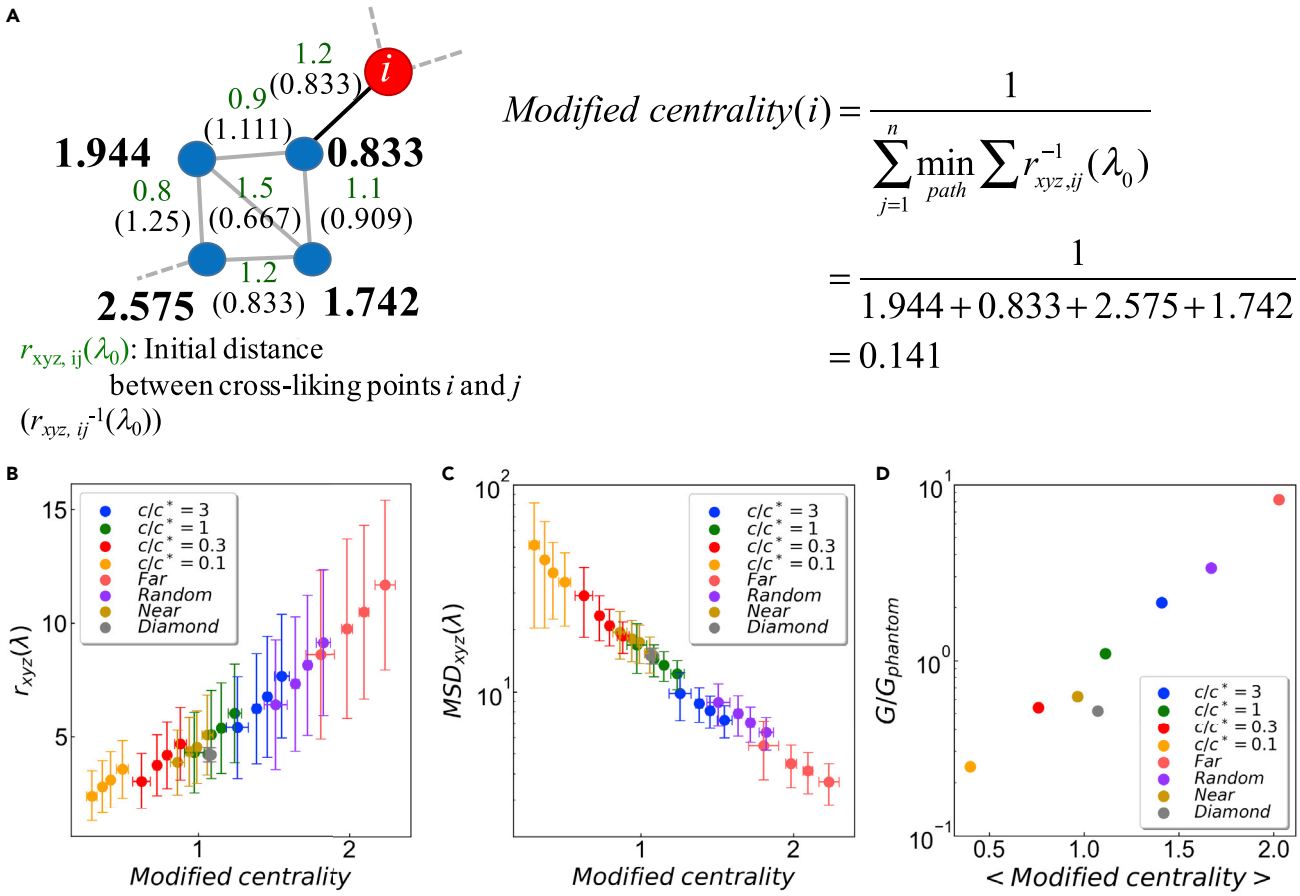

Figure 4. Universal Description of $r_{xyz}(\lambda)$ and $MSD_{xyz}(\lambda)$ Using Modified Centrality

(A) The closeness centrality $C_c(\lambda_0)$ is the reciprocal of the sum of the weights of the shortest paths between any node and all other nodes (Figure S6). In terms of modified centrality, the weight is $r_{xyz,ij}^{-1}(\lambda_0)$ instead of 1 for the closeness centrality. The $r_{xyz}(\lambda_0)$ values shown in this figure are arbitrary numbers used for the explanation, and the calculation example is shown in a limited region.

(B and C) (B) $r_{xyz}(\lambda)$ and (C) $MSD_{xyz}(\lambda)$ are the functions of the modified centrality of synthetically and randomly crosslinked elastomers at $\lambda = 2$.

(D) Relationship between shear modulus and modified centrality. The modulus was calculated from the plateau region on a Mooney-Rivlin plot. Blue, green, red, and orange circles represent the synthetically crosslinked polymers prepared at $c/c^* = 3$, 1, 0.3, and 0.1, respectively. Pink, purple, yellow ochre, and gray circles represent the far, random, and near conditions and the diamond-like network, respectively.

of the sum of the inverse of the end-to-end distance for all shortest paths between *i* and all other nodes (Figure 4A). The resulting modified centrality was related to both $r_{xyz}(\lambda)$ and $MSD_{xyz}(\lambda)$ in both synthetically and randomly crosslinked elastomers (Tables S7 and S8). Except for the diamond-like elastomers, these plots were mostly located on a single line, thereby suggesting that modified centrality could be an essential parameter for the mechanical properties of heterogeneous elastomer networks (Figures 4B and 4C). Although the correlation coefficient was occasionally lower than that of $r_{xyz}(\lambda_0)$ and $C_c(\lambda_0)$, the universal description for both $r_{xyz}(\lambda)$ and $MSD_{xyz}(\lambda)$ is meaningful. Thus, the parameters with topological and spatial information may be essential for global stress through the fluctuation and expansion of the crosslinking points. Furthermore, we tried to improve the modified centrality. Instead of the inverse of the distance between crosslinking points or nodes, inverses of square or root of the distance were introduced into the weight of the links. The correlation coefficients were improved in some cases (Tables S9–S12), and the plot was not on linear lines (Figure S11). Hence, it is possible that these network indicators, with several ways of incorporating the distances between nodes, might be predictable to other objectives. The foregoing results indicate that the modified centrality can be a superior descriptor representing the mesoscopic structure of heterogeneous elastomers for a description of the mechanical properties.

The modified centrality includes both topological and spatial information. With an increase in modified centrality, the crosslinking point is positioned in a central network, or the neighboring crosslinked points are located at distant locations. Therefore, it is possible that when the modified centrality is increased, the fluctuation of the crosslinking points is suppressed. As mentioned above, the expansion of the end-to-end distance can follow an elongation of the entire matrix with increasing initial distance. As a result, the modified centrality can affect both the fluctuation of the crosslinked points and an expansion of the end-to-end distance, which can alter global stress. This interpretation may be supported by a clear relationship between the average modified centrality and the shear moduli of both synthetically and

randomly crosslinked elastomers (Figure 4D). Another perspective is the scale effect of centrality. Because the centrality decreases with an increase in the number of nodes, the number of polymers was fixed at $N_{xlp} = 100$ for the foregoing discussion. With an increase in size, a decrease in the centrality and a clearer correlation were observed (Figure S12). We will report the details regarding the size effect in a future study that addresses the current limitations of our machine resources.

From the viewpoint of complex network science, a method to incorporate spatial distance into network indicators was demonstrated herein. Generally, in complex network science the indicator mainly focuses on the connectivity or relationship between nodes. On the other hand, there have been attempts to incorporate the spatial distance into a topological network, which is known as a spatial network.[43] Previously it was reported that closeness centrality in the spatial network was estimated by introducing spatial distance into the shortest paths between nodes, whereby a shorter distance reflected a stronger relationship.[44] In our case, the inverse of the distance between neighbor nodes was translated into the weight of each link to calculate the closeness centrality in the spatial network. This approach might be useful when a longer distance or higher values indicate closer relationships. For example, the inverse of conversation time could be incorporated in the weight of the link in a human network, whereby a longer conversation time would reflect a closer relationship. Thus, the methodology to obtain the modified centrality might contribute not only to materials science but also to other fields.

Conclusions

In this study, we demonstrated a novel approach in terms of describing the structure-property relationships of elastomers using a complex network. We found that network centrality with topological and spatial information should be a novel mesoscopic descriptor for heterogeneous elastomers to describe the mechanical properties. Considering that the complex network provides quantitative information on each node in an entire network, the roles of each crosslinking point could be individually assigned. It should be noted that our descriptor was linearly correlated with some parameters that determine mechanical properties, such as end-to-end distance and the fluctuation of crosslinked points. The method of extracting the mesoscopic descriptor from the network of elastomers prior to elongations could afford high generality and interpretability to predict the stresses under elongations. These results highlight a new way to describe the fundamental relationship between a network structure at the mesoscopic scale and the mechanical properties of elastomers. Another perspective is the development of a method to incorporate distance information into closeness centrality. There should be several cases in which the network indicator should consider the spatial distance between nodes to explain any objective.

Our next task is to apply our system to elastomers with more complex connectivity, such as networks with different numbers of particles between crosslinking points prepared by chain-growth polymerization or with different numbers of branching. The issues related to the foregoing should be addressed for the development of a superior mesoscopic descriptor indicating stronger correlation than the current baseline with moderate correlation coefficients. Furthermore, the combination with experimental techniques should be attempted in future tasks for the purpose of developing new materials with desired properties. Recently, experimental techniques to measure mesoscale mechanical properties, such as nanorheological atomic force microscopy, have been developed.[45] The combination with experiments enables us to optimize not only stress but also other important mechanical properties, such as a fracture. We hope that our method for extracting mesoscopic descriptors can later be applied to other materials with a network structure.

EXPERIMENTAL PROCEDURES

Resource Availability

Lead Contact

Yoshifumi Amamoto is the Lead Contact of this study and can be reached by e-mail: y-amamoto@ms.ifoc.kyushu-u.ac.jp.

Materials Availability

This study did not generate new unique reagents.

Data and Code Availability

Simulation raw data and the intermediate data and scripts that are needed to draw main figures are available from Mendeley Data at 10.17632/d8fh6ty4mh.2.

SUPPLEMENTAL INFORMATION

Supplemental Information can be found online at https://doi.org/10.1016/j.patter.2020.100135.

ACKNOWLEDGMENTS

We would like to thank JSOL for their fruitful discussion of the J-OCTA software. Prof. M. Doi, Prof. T. Sakai, Dr. T. Katashima, and Dr. N. Sakumichi are acknowledged for their helpful discussions. The computer resources were partially supported based on the category of General Projects by the Research Institute for Information Technology, Kyushu University, and by the Initiative on Promotion of Supercomputing for Young or Women Researchers at the Information Technology Center from the University of Tokyo. This work is supported by the "Joint Usage/Research Center for Interdisciplinary Large-scale Information Infrastructures" and the "High Performance Computing Infrastructure" in Japan (Project ID: jh200016-NAH). This work was also supported by the JSPS Grant-in-Aid for Scientific Research on Innovative Areas, Discrete Geometric Analysis for Materials Design: 17H06460 (steering group), 17H06468, 18H04483, and 20H04644, by a Grant-in-Aid for Scientific Research (A): 17H01152, by the Grant-in-Aid for Scientific Research (B): 20H02800, and by Early-Career Scientists: 18K14273 from JSPS. Y.A. acknowledges the financial support of the Grant-in-Aid for Research Fellows from JSPS (15J12397).

AUTHOR CONTRIBUTIONS

Y.A. carried out the simulation, analyzed the data, and wrote the manuscript. Y.A. and T.O. designed our analytical method for elastomers based on a complex network. Y.M. and T.O. supervised the simulation and complex network, respectively. All authors discussed contributed to the interpretation of the results and commented on the manuscript.

DECLARATION OF INTERESTS

The authors declare no competing interests.

Received: June 15, 2020
Revised: August 25, 2020
Accepted: September 30, 2020
Published: October 28, 2020

REFERENCES

1. Fujita, D., Ueda, Y., Sato, S., Mizuno, N., Kumasaka, T., and Fujita, M. (2016). Self-assembly of tetravalent Goldberg polyhedra from 144 small components. Nature *540*, 563–566.
2. Ichinomiya, T., Obayashi, I., and Hiraoka, Y. (2017). Persistent homology analysis of craze formation. Phys. Rev. E *95*, 012504.
3. Jackson, N.E., Webb, M.A., and de Pablo, J.J. (2019). Recent advances in machine learning towards multiscale soft materials design. Curr. Opin. Chem. Eng. *23*, 106–114.
4. Pokuri, B.S.S., Ghosal, S., Kokate, A., Sarkar, S., and Ganapathysubramanian, B. (2019). Interpretable deep learning for guided microstructure-property explorations in photovoltaics. NPJ Comput. Mater. *5*, 95.
5. Wang, W.J., and Gomez-Bombarelli, R. (2019). Coarse-graining auto-encoders for molecular dynamics. NPJ Comput. Mater. *5*, 125.
6. Urayama, K., and Kohjiya, S. (1996). Crossover of the concentration dependence of swelling and elastic properties for polysiloxane networks crosslinked in solution. J. Chem. Phys. *104*, 3352–3359.
7. Norisuye, T., Masui, N., Kida, Y., Ikuta, D., Kokufuta, E., Ito, S., Panyukov, S., and Shibayama, M. (2002). Small angle neutron scattering studies on structural inhomogeneities in polymer gels: irradiation cross-linked gels vs chemically cross-linked gels. Polymer *43*, 5289–5297.
8. Urayama, K. (2006). An experimentalist's view of the physics of rubber elasticity. J. Polym. Sci. Pol. Phys. *44*, 3440–3444.
9. Svaneborg, C., Everaers, R., Grest, G.S., and Curro, J.G. (2008). Connectivity and entanglement stress contributions in strained polymer networks. Macromolecules *41*, 4920–4928.
10. Amamoto, Y., Otsuka, H., Takahara, A., and Matyjaszewski, K. (2012). Changes in network structure of chemical gels controlled by solvent quality through photoinduced radical reshuffling reactions of trithiocarbonate units. ACS Macro Lett. *1*, 478–481.
11. Kuhn, W., and Grun, F. (1942). Relations between elastic constants and the strain birefringence of high-elastic substances. Kolloid Z. *101*, 248–271.
12. Treloar, L.R.G. (1944). Stress-strain data for vulcanised rubber under various types of deformation. T Faraday Soc. *40*, 0059–0069.
13. Kubo, R. (1947). Statistical theory of linear polymers .2. Elasticity of vulcanized rubber. J. Phys. Soc. Jpn. *2*, 51–56.
14. Treloar, L.R.G. (1949). The Physics of Rubber Elasticity (Clarendon Press).
15. Wall, F.T., and Flory, P.J. (1951). Statistical thermodynamics of rubber elasticity. J. Chem. Phys. *19*, 1435–1439.
16. James, H.M., and Guth, E. (1953). Statistical thermodynamics of rubber elasticity. J. Chem. Phys. *21*, 1039–1049.
17. Doi, M. (2013). Soft Matter Physics, First Edition (Oxford University Press).
18. Li, C.Y., and Strachan, A. (2015). Molecular scale simulations on thermoset polymers: a review. J. Polym. Sci. Pol. Phys. *53*, 103–122.
19. Miller, D.R., and Macosko, C.W. (1976). New derivation of post gel properties of network polymers. Macromolecules *9*, 206–211.
20. Edwards, S.F., and Vilgis, T. (1986). The effect of entanglements in rubber elasticity. Polymer *27*, 483–492.
21. Everaers, R., and Kremer, K. (1996). Topological interactions in model polymer networks. Phys. Rev. E *53*, 37–40.
22. Panyukov, S., and Rabin, Y. (1996). Statistical physics of polymer gels. Phys. Rep. *269*, 1–131.
23. Everaers, R. (1999). Entanglement effects in defect-free model polymer networks. New J. Phys. *1*, https://doi.org/10.1088/1367-2630/1/1/312.
24. Rubinstein, M., and Panyukov, S. (2002). Elasticity of polymer networks. Macromolecules *35*, 6670–6686.
25. Shokuhfar, A., and Arab, B. (2013). The effect of cross linking density on the mechanical properties and structure of the epoxy polymers: molecular dynamics simulation. J. Mol. Model. *19*, 3719–3731.
26. Zhong, M.J., Wang, R., Kawamoto, K., Olsen, B.D., and Johnson, J.A. (2016). Quantifying the impact of molecular defects on polymer network elasticity. Science *353*, 1264–1268.
27. Panyukov, S. (2019). Loops in polymer networks. Macromolecules *52*, 4145–4153.
28. Chea, E., and Livesay, D.R. (2007). How accurate and statistically robust are catalytic site predictions based on closeness centrality? BMC Bioinformatics *8*, 153.
29. Okamoto, K., Chen, W., and Li, X.Y. (2008). Ranking of closeness centrality for large-scale social networks. Lect Notes Comput. Sci. *5059*, 186–195.
30. Ohnishi, T., Takayasu, H., and Takayasu, M. (2009). Hubs and authorities on Japanese inter-firm network: characterization of nodes in very large directed networks. Prog. Theor. Phys. Supp. *179*, 157–166.
31. Liu, Y.Y., Slotine, J.J., and Barabasi, A.L. (2011). Controllability of complex networks. Nature *473*, 167–173.
32. Semenov, M., and Lelushkina, K. (2016). Study of the materials microstructure using topological properties of complex networks. Iop Conf. Ser Mat. Sci. *135*, 012040.
33. Dehmamy, N., Milanlouei, S., and Barabasi, A.L. (2018). A structural transition in physical networks. Nature *563*, 676–680.
34. Kryven, I., Duivenvoorden, J., Hermans, J., and Iedema, P.D. (2016). Random graph approach to multifunctional molecular networks. Macromol Theor. Simul *25*, 449–465.
35. Duering, E.R., Kremer, K., and Grest, G.S. (1991). Relaxation of randomly cross-linked polymer melts. Phys. Rev. Lett. *67*, 3531–3534.
36. Duering, E.R., Kremer, K., and Grest, G.S. (1994). Structure and relaxation of end-linked polymer networks. J. Chem. Phys. *101*, 8169–8192.
37. Hoy, R.S., and O'Hern, C.S. (2010). Viscoplasticity and large-scale chain relaxation in glassy-polymeric strain hardening. Phys. Rev. E *82*, 041803.
38. Sakai, T., Matsunaga, T., Yamamoto, Y., Ito, C., Yoshida, R., Suzuki, S., Sasaki, N., Shibayama, M., and Chung, U.I. (2008). Design and fabrication of a high-strength hydrogel with ideally homogeneous network structure from tetrahedron-like macromonomers. Macromolecules *41*, 5379–5384.
39. Akagi, Y., Katashima, T., Katsumoto, Y., Fujii, K., Matsunaga, T., Chung, U., Shibayama, M., and Sakai, T. (2011). Examination of the theories of rubber elasticity using an ideal polymer network. Macromolecules *44*, 5817–5821.
40. Takagi, K., Murayama, S., Sakai, T., Asai, M., Santa, T., and Kato, M. (2014). A computer simulation of the networked structure of a hydrogel prepared from a tetra-armed star pre-polymer. Soft Matter *10*, 3553–3559.
41. Obukhov, S.P., Rubinstein, M., and Colby, R.H. (1994). Network modulus and superelasticity. Macromolecules *27*, 3191–3198.
42. Miehe, C., Goktepe, S., and Lulei, F. (2004). A micro-macro approach to rubber-like materials—part I: the non-affine micro-sphere model of rubber elasticity. J. Mech. Phys. Sol. *52*, 2617–2660.
43. Barthélemy, M. (2011). Spatial networks. Phys. Rep. *499*, 1–101.
44. Crucitti, P., Latora, V., and Porta, S. (2006). Centrality measures in spatial networks of urban streets. Phys. Rev. E *73*, 036125.
45. Hosoya, R., Morita, H., and Nakajima, K. (2020). Analysis of nanomechanical properties of polyethylene using molecular dynamics simulation. Macromolecules *53*, 6163–6172.